Journal of Engineering Mathematics 22: 123–142 (1988)

Local error analysis in 3-D panel methods

J.E. ROMATE
Netherlands Technology Foundation, c/o Delft Hydraulics, P.O. Box 152, 8300 AD Emmeloord, The Netherlands

Received 15 September 1987; accepted 11 November 1987

Abstract. In this paper a local error analysis is given of the approximation of the integrals used in boundary integral equation methods for solving Laplace's equation. Using Taylor series expansions approximate expressions are derived for the velocity and velocity-potential integrals. The asymptotic behaviour of the local truncation error is given in terms of the panel grid size.

1. Introduction

To describe the irrotational flow of an inviscid, incompressible fluid a velocity potential ϕ is introduced where the fluid velocity $\mathbf{v}$ is given by $\mathbf{v} = \nabla\phi$. The potential ϕ then satisfies Laplace's equation throughout the fluid domain Ω:

$$\nabla^2\phi(\mathbf{x}) = 0, \quad \mathbf{x} \in \Omega, \tag{1.1}$$

and is subject to boundary conditions

$$f\left(\mathbf{x}, t, \phi, \frac{\partial\phi}{\partial n}, \ldots\right) = 0, \quad \mathbf{x} \in S. \tag{1.1a}$$

Panel methods (or: boundary element methods, boundary integral equation methods) have been used for solving potential flow problems since the early sixties (see e.g., [1]). In these methods the boundary value problem (1.1) – (1.1a) is solved by means of integral equations, based on Green's third identity, where the integration is over the boundary S of the fluid domain Ω.

In this paper we will consider integral equations expressing the velocity and the velocity potential in a point $\mathbf{x}$ in terms of a source distribution σ and a dipole distribution μ on the boundary S:

$$\phi(\mathbf{x}) = \iint_S - \left(\sigma \frac{1}{r} + \mu \frac{\mathbf{n}\cdot\mathbf{r}}{r^3}\right) \mathrm{d}S, \quad \mathbf{x} \in S, \tag{1.2}$$

$$\mathbf{v}(\mathbf{x}) = \iint_S - \left(\sigma\nabla_x\left(\frac{1}{r}\right) + \mu\nabla_x\left(\frac{\mathbf{n}\cdot\mathbf{r}}{r^3}\right)\right) \mathrm{d}S, \quad \mathbf{x} \in S, \tag{1.3}$$

where ∇_x denotes the gradient operator $(\partial/\partial x, \partial/\partial y, \partial/\partial z)^T$. The major advantage of panel methods is that the computational domain (here the boundary S) has a dimension which

is one lower than that of the computational domain of field discretization methods which involve the discretization of the entire domain Ω. Due to this attractive feature, panel methods have become more widespread in the last 15–20 years, and now numerous versions have been developed, both in 2 and 3 dimensions (see e.g., [2]). Most common are the lower-order methods, where the boundary S of the fluid domain is approximated by flat panels or elements. On each element the singularity distributions (source and/or dipole) are taken to be constant. More recently also higher-order methods have been developed to circumvent some of the disadvantages of the lower-order methods, such as low accuracy and singular behavior at panel edges. These methods take curvature effects into account and use piecewise linear or quadratic singularity distributions [6].

The accuracy of the approximation of the boundary integrals determines the discretization error. Therefore it is important to have an a priori estimate of the order of the global error when using a given approximation of the geometry and the singularity distributions. However, the mathematics involved in deducing such global error estimates is very complicated, and general results on the accuracy and asymptotic convergence of panel methods are not yet available, this in spite of important progress made by, for instance, Wendland [3] and Schippers [4]. A very different approach was given by Hess in a series of papers (see e.g., [5]) in which he used a small-curvature expansion to obtain locally consistent approximations of velocity integrals.

Here we will pursue the local error analysis method of Hess further to derive consistent approximations for both velocity and velocity-potential integrals in three dimensions. Giving estimates of the asymptotic behavior of the leading terms in the expansions it is indicated which contributions should be taken into account to obtain local truncation errors of various orders in terms of the characteristic panel grid size Δ. In this analysis we will give approximations with truncation errors up to $O(\Delta^3)$ for the velocity potential, and up to $O(\Delta^2)$ for the velocity. One should bear in mind that in most applications only the velocity (and the pressure) is of interest, and not the potential. Therefore, when using the potential equation (1.2), the potential will be differentiated to obtain the velocity. This means that in order to have an $O(\Delta^n)$-truncation error for the velocity, the potential has to be approximated up to $O(\Delta^{n+1})$. All the integrals in the expansions can be calculated analytically without the use of numerical quadrature. This is an important advantage since due to the singular kernels of the integrals numerical quadrature can give bad results in the near field (when the field point $\mathbf{x}$ is near the panel). Since most of the computing time in panel methods is spent on the calculation of these integrals it is important to minimize the amount of work to get the desired accuracy. Therefore we will also consider the truncation errors of the multipole expansions used for far-field approximations.

2. Surface geometry and discretization

Consider a C^2-continuous surface S described by the following parametrization:

$$\mathbf{x} = \mathbf{x}(u, v) \tag{2.1}$$

where $(u, v) \in [0, u_{\max}] \times [0, v_{\max}]$. The surface is discretized in panels by discretizing the parameter domain into rectangular panels bounded by lines of constant u and v. On each panel $(u, v) \in [u_i, u_{i+1}] \times [v_j, v_{j+1}]$ an expansion point (u_0, v_0) is chosen such that the point

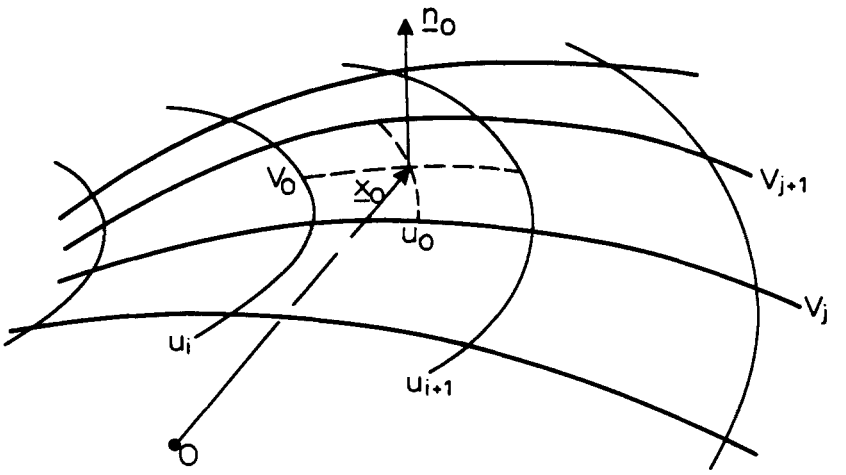

Fig. 1. Surface approximation.

$\mathbf{x}_0(u_0, v_0)$ in physical space is near the centre of the panel (Fig. 1). Now, the integrals over S are expressed as the sum of the integrals over all N panel surfaces ΔS_i, so that we can replace (1.2) and (1.3) by the expressions:

$$\phi(\mathbf{x}) = \sum_{i=1}^{N} \iint_{\Delta S_i} -\left(\sigma \frac{1}{r} + \mu \frac{\mathbf{n}\cdot\mathbf{r}}{r^3}\right) \mathrm{d}S, \qquad \mathbf{x} \in S, \tag{2.2}$$

$$\mathbf{v}(\mathbf{x}) = \sum_{i=1}^{N} \iint_{\Delta S_i} -\left(\sigma \nabla_x\left(\frac{1}{r}\right) + \mu \nabla_x\left(\frac{\mathbf{n}\cdot\mathbf{r}}{r^3}\right)\right) \mathrm{d}S, \quad \mathbf{x} \in S. \tag{2.3}$$

Unfortunately the integrals over the panel surfaces can not be calculated exactly. Obviously some approximation has to be made to the singularity distributions σ and μ over a panel, but also an approximation has to be made of the panel surface ΔS. Here we want to investigate the contribution of one panel ΔS in (2.2) and (2.3) to the truncation error involved using these approximations.

To facilitate the calculations we introduce a local orthonormal panel coordinate system on ΔS with origin at $\mathbf{x}_0(u_0, v_0)$ and unit vectors $\mathbf{e}_1$, $\mathbf{e}_2$ and $\mathbf{e}_3$, where $\mathbf{e}_3 = \mathbf{n}$ (the local normal vector at $\mathbf{x}_0$) and $\mathbf{e}_1$ and $\mathbf{e}_2$ are tangent to the surface at $\mathbf{x}_0$ (Fig. 2). Expressed in these local panel coordinates we will thus consider the following integrals:

$$\phi_s(\mathbf{x}) = -\iint_{\Delta S} \sigma \frac{1}{r} \mathrm{d}S, \tag{2.4}$$

$$\mathbf{v}_s(\mathbf{x}) = -\iint_{\Delta S} \sigma \nabla_x\left(\frac{1}{r}\right) \mathrm{d}S, \tag{2.5}$$

$$\phi_d(\mathbf{x}) = -\iint_{\Delta S} \mu \frac{\mathbf{n}\cdot\mathbf{r}}{r^3} \mathrm{d}S, \tag{2.6}$$

$$\mathbf{v}_d(\mathbf{x}) = -\iint_{\Delta S} \mu \nabla_x\left(\frac{\mathbf{n}\cdot\mathbf{r}}{r^3}\right) \mathrm{d}S. \tag{2.7}$$

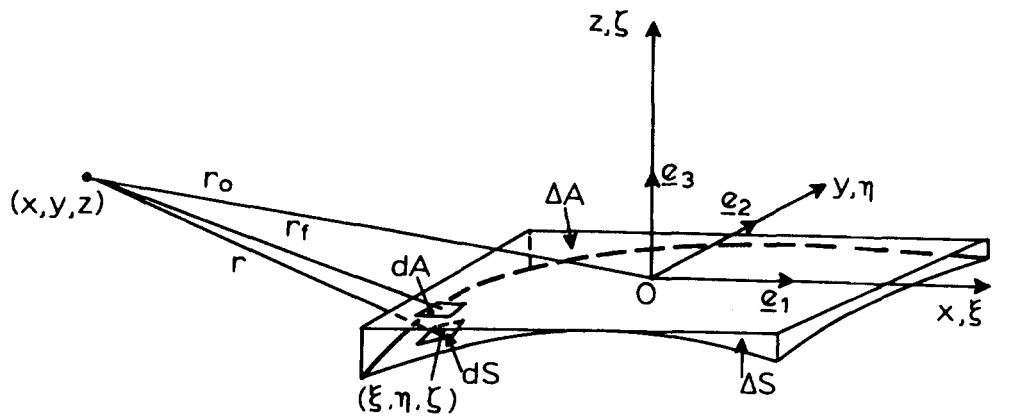

Fig. 2. Local panel coordinate system.

The integration variable will be denoted by $\xi = (\xi, \eta, \zeta)$ (on ΔS), so that $\sigma = \sigma(\xi)$, $\mu = \mu(\xi)$, and $\mathbf{n} = \mathbf{n}(\xi)$, the normal at ξ. The distance $r = |\mathbf{r}| = |\mathbf{x} - \xi|$ is the distance between the field point $\mathbf{x}$ and ξ on ΔS.

3. Geometric expansions; assumptions

To evaluate equations (2.4)–(2.7) the integrals are approximated using Taylor series expansions for σ, μ and the panel surface. It is assumed that the panel surface can be expressed as

$$\zeta = \zeta(\xi, \eta). \tag{3.1}$$

Now, using the origin $\mathbf{x}_0$ of the panel coordinate system as expansion point, $\sigma(\xi)$ and $\mu(\xi)$ can be expanded as follows:

$$\begin{aligned}\sigma(\xi) &= \sigma_0 + (\sigma_x\xi + \sigma_y\eta) + (\tfrac{1}{2}\sigma_{xx}\xi^2 + \sigma_{xy}\xi\eta + \tfrac{1}{2}\sigma_y\eta^2) + \ldots \\ &= \sigma_0 + \sigma_1 + \sigma_2 + O(\Delta^3),\end{aligned} \tag{3.2}$$

$$\begin{aligned}\mu(\xi) &= \mu_0 + (\mu_x\xi + \mu_y\eta) + (\tfrac{1}{2}\mu_{xx}\xi^2 + \mu_{xy}\xi\eta + \tfrac{1}{2}\mu_{yy}\eta^2) + \ldots \\ &= \mu_0 + \mu_1 + \mu_2 + O(\Delta^3),\end{aligned} \tag{3.3}$$

where Δ is the characteristic panel size ($\Delta \ll 1$). Here it is assumed that $\sigma_0, \sigma_x, \sigma_y, \ldots, \mu_0, \mu_x, \mu_y, \mu_{xx}, \ldots$ are of O(1), so that σ_0 and μ_0 are O(1), σ_1 and μ_1 are O(Δ), and more general σ_n and μ_n are O(Δ^n).

The panel surface can be expressed as (Fig. 2)

$$\begin{aligned}\zeta(\xi, \eta) &= (c_{xx}\xi^2 + c_{xy}\xi\eta + c_{yy}\eta^2) + (T_{30}\xi^3 + T_{21}\xi^2\eta + T_{12}\xi\eta^2 + T_{03}\eta^3) + \ldots \\ &= \zeta_2 + \zeta_3 + O(\Delta^4),\end{aligned} \tag{3.4}$$

or

$$F(\xi, \eta, \zeta) = \zeta - \zeta_2 - \zeta_3 - \cdots = 0. \tag{3.5}$$

Then the unit normal $\mathbf{n}$ is panel coordinates on ΔS is

$$\mathbf{n} = \frac{\nabla F}{|\nabla F|}, \tag{3.6}$$

It is assumed that the curvature and twist coefficients c_{xx}, c_{xy}, . . . are at most O(1).

Now the integration will be over the area ΔA, which is the projection of ΔS along $\mathbf{e}_3$ on the $\xi\eta$-plane. (Notice that in general the boundaries of ΔA are curved). Clearly, the panel area ΔS is $O(\Delta^2)$.

Using the panel surface expansion (3.4) we can expand all $\boldsymbol{\xi}$-dependent quantities in the integrals (2.4)–(2.7). In the first place dS can be written as

$$dS = \frac{1}{\mathbf{n} \cdot \mathbf{e}_3} dA = [1 + \tfrac{1}{2}[\zeta_{2\xi}^2 + \zeta_{2\eta}^2) + O(\Delta^3)] \, d\xi \, d\eta. \tag{3.7}$$

Secondly, we write (Fig. 2):

$$\mathbf{r} = \mathbf{r}_f - \zeta \mathbf{e}_3, \; r_f = |\mathbf{r}_f| \quad \text{(Euclidean norm)} \tag{3.8}$$

where in the near field $r_f = O(\Delta)$, and in the far field $r_f = O(1)$. Furthermore,

$$r = O(r_f), \quad x - \xi = O(r_f), \quad y - \eta = O(r_f), \quad \zeta = O(\Delta^2), \quad \xi, \eta = O(\Delta).$$

The order of magnitude of z is more subtle. In general $z = O(r_f)$. However, if $\mathbf{x} = (x, y, z)^T$ is on the same C^2-continuous surface S as the panel is, and $\mathbf{x}$ is in the near field, then z can be expressed as

$$z = c_{xx}x^2 + c_{xy}xy + c_{yy}y^2 + O(r_f)^3, \tag{3.10}$$

showing z to be $O(r_f^2) = O(\Delta^2)$ in this case. Thus, when the entire boundary S is C^2-continuous, z will always be $O(\Delta^2)$ in the near field. But since in general the boundary S will not be smooth but will contain corners and edges, we will assume z to be only $O(r_f) = O(\Delta)$ in the near field.

Using (3.8) and the assumptions mentioned above we will use the following expansion of $1/r^k$ for the near field:

$$\frac{1}{r^k} = \frac{1}{r_f^k}\left(1 + \frac{kz\zeta_2}{r_f^2} + \left(\frac{kz\zeta_3}{r_f^2} + \left(\frac{k(k+2)}{2}\frac{z^2}{r_f^2} - \frac{k}{2}\right)\frac{\zeta_2^2}{r_f^2}\right) + \cdots\right)$$

$$= \frac{1}{r_f^k}[1 + C_{k1} + C_{k2} + O(\Delta^3)], \tag{3.11}$$

where

$$C_{k1} = O\left(\frac{z\Delta^2}{r_f^2}\right) = O(\Delta),$$

$$C_{k2} = O\left(\frac{z\Delta^3}{r_f^2}, \frac{z^2\Delta^4}{r_f^4}, \frac{\Delta^4}{r_f^2}\right) = O(\Delta^2).$$

Although this expansion is valid for both near field and far field we will not use (3.11) in the far field, but use (Fig. 2)

$$\frac{1}{r^k} = \frac{1}{r_0^k}(1 + O(\Delta)) \tag{3.12}$$

instead. Here r_0 is the distance between the field point and the panel centre. This leads to the often used multipole expansions, where integrals M_{kl} are involved defined by

$$M_{kl} = \iint_{\Delta S} \xi^k \eta^l \, d\xi \, d\eta \tag{3.13}$$

with $M_{00} = O(\Delta^2)$, and M_{10} and M_{01} of $O(\Delta^4)$.

In the next sections we will derive small-curvature expansions for (2.4)–(2.7) for the near field, and present multipole approximations for the far field.

4. Potential due to a source distribution

Near field $r_f = O(\Delta)$

The potential ϕ_s in $\mathbf{x}$ due to a source distribution $\sigma(\xi)$ on a panel ΔS is given by

$$\phi_s(\mathbf{x}) = -\iint_{\Delta S} \sigma(\xi) \frac{1}{r} \, dS. \tag{4.1}$$

Expanding the integral gives

$$\phi_s(\mathbf{x}) = \iint_{\Delta S} \frac{-1}{r_f} [(1 + C_{11} + C_{12} + \ldots)(\sigma_0 + \sigma_1 + \sigma_2 + \ldots)$$

$$(1 + \tfrac{1}{2}(\zeta_{2\xi}^2 + \zeta_{2\eta}^2) + \ldots)] \, dA = I_1 + (I_2 + I_3) + O(\Delta^3). \tag{4.2}$$

The orders of magnitude of the 3 lowest-order terms are

$$I_1 = -\iint_{\Delta S} \frac{1}{r_f} \sigma_0 \, dA, \qquad = O\left(\frac{1}{r_f}\Delta^2\right) = O(\Delta),$$

$$I_2 = -\iint_{\Delta S} \frac{1}{r_f} \sigma_1 \, dA, \qquad = O\left(\frac{1}{r_f}\Delta^3\right) = O(\Delta^2), \tag{4.3}$$

$$I_3 = -\iint_{\Delta S} \frac{1}{r_f}\sigma_0 C_{11}\,\mathrm{d}A, \quad = \mathrm{O}\left(\frac{1}{r_f}\frac{z\Delta^2}{r_f^2}\Delta^2\right) = \mathrm{O}(\Delta^2).$$

Thus we see that to obtain a local truncation error of $\mathrm{O}(\Delta^2)$ only I_1 has to be calculated. I_1 represents the potential $\phi_s(\mathbf{x})$ due to a constant source distribution over a flat panel. To obtain a cubic truncation error in Δ, a linear source distribution is needed (σ_1 in I_2) and also the curvature of the panel has to be taken into account (C_{11} in I_3). A higher-order truncation error than $\mathrm{O}(\Delta^3)$ would involve at least a quadratic source distribution and a cubic surface representation. In this analysis, however, we will only consider truncation errors up to $\mathrm{O}(\Delta^3)$ for the velocity potential.

Far field: $r_f = \mathrm{O}(1)$

Expanding (4.1), now using (3.12), gives

$$\phi_s(\mathbf{x}) = \iint_{\Delta S} \frac{-\sigma_0}{r_0}\,\mathrm{d}A + \mathrm{O}(\Delta^4) = \frac{-\sigma_0}{r_0} M_{00} + \mathrm{O}(\Delta^4). \tag{4.4}$$

5. Velocity due to a source distribution

Near field: $r_f = \mathrm{O}(\Delta)$

The velocity $\mathbf{v}_s$ in $\mathbf{x}$ due to a surface source distribution $\sigma(\boldsymbol{\xi})$ on a panel ΔS is given by

$$\mathbf{v}_s(\mathbf{x}) = -\iint_{\Delta S} \sigma(\boldsymbol{\xi})\,\nabla_x\left(\frac{1}{r}\right)\mathrm{d}S = \iint_{\Delta S} \sigma(\boldsymbol{\xi})\frac{\mathbf{r}}{r^3}\,\mathrm{d}S \tag{5.1}$$

$$= \iint_{\Delta S} \frac{1}{r_f^3}(1 + C_{31} + C_{32} + \ldots)(\sigma_0 + \sigma_1 + \ldots)$$

$$(1 + \mathrm{O}(\Delta^2))(\mathbf{r}_f - \zeta\mathbf{e}_3)\,\mathrm{d}A = \mathbf{J}_1 + (\mathbf{J}_2 + \mathbf{J}_3 + \mathbf{J}_4) + \mathrm{O}(\Delta^2).$$

The lowest-order contributions have the following order of magnitude:

$$\mathbf{J}_1 = \iint_{\Delta S} \frac{1}{r_f^3}\sigma_0\mathbf{r}_f\,\mathrm{d}A = \mathrm{O}(1),$$

$$\mathbf{J}_2 = \iint_{\Delta S} \frac{1}{r_f^3}\sigma_0(-\zeta_2)\mathbf{e}_3\,\mathrm{d}A = \mathrm{O}(\Delta),$$

$$\mathbf{J}_3 = \iint_{\Delta S} \frac{1}{r_f^3}\sigma_1\mathbf{r}_f\,\mathrm{d}A = \mathrm{O}(\Delta), \tag{5.2}$$

$$\mathbf{J}_4 = \iint_{\Delta S} \frac{1}{r_f^3}\sigma_0 C_{31}\mathbf{r}_f\,\mathrm{d}A = \mathrm{O}(\Delta).$$

Comparison with (4.3) shows that when the same approximation of source distribution and panel geometry is used, the truncation error of the velocity approximation is $O(1/\Delta)$ times the truncation error of the potential approximation, due to the application of the gradient operator. Thus we see that for a given source and panel-surface approximation the same order of truncation error is obtained for the velocity, whether one uses (5.1) directly, or uses (4.1) instead and calculates the velocity from ϕ_s using numerical differentiation.

Far field: $r_f = O(1)$

In this case expanding (5.1) gives

$$\mathbf{v}_s(\mathbf{x}) = \iint_{\Delta S} \sigma \frac{\mathbf{r}}{r^3} \, dS = \iint_{\Delta S} \frac{\sigma_0}{r_0^3} \mathbf{x} \, dA + \ldots$$

$$= \frac{\sigma_0}{r_0^3} M_{00}\mathbf{x} + O(\Delta^4). \tag{5.3}$$

6. Velocity due to a dipole distribution

Near field: $r_f = O(\Delta)$

The velocity due to a surface dipole distribution is given by

$$\mathbf{v}_d(\mathbf{x}) = -\iint_{\Delta S} \mu \nabla_x \left(\frac{\mathbf{n} \cdot \mathbf{r}}{r^3} \right) dS$$

$$= \iint_{\Delta S} \boldsymbol{\gamma} \times \frac{\mathbf{r}}{r^3} \, dS - \oint_c \mu \frac{\mathbf{r} \times \mathbf{dl}}{r^3} = \mathbf{v}_v + \mathbf{v}_{lv} \tag{6.1}$$

where $\boldsymbol{\gamma} = \nabla\mu \times \mathbf{n}$, $\mathbf{n} = (n_1, n_2, n_3)^T$. That is, the velocity is expressed in terms of a surface vortex distribution $\boldsymbol{\gamma}$ and a line vortex μ along the perimeter $C = \Sigma_i C_i$ of ΔS (the perimeter-parts C_i are assumed to be C^2-continuous).

Now

$$\boldsymbol{\gamma} = \nabla\mu \times \mathbf{n} = \begin{pmatrix} \gamma_1 \\ \gamma_2 \\ \gamma_3 \end{pmatrix} = \begin{pmatrix} \dfrac{\partial \mu}{\partial \eta} n_3 \\ -\dfrac{\partial \mu}{\partial \xi} n_3 \\ \dfrac{\partial \mu}{\partial \xi} n_2 - \dfrac{\partial \mu}{\partial \eta} n_1 \end{pmatrix}, \tag{6.2}$$

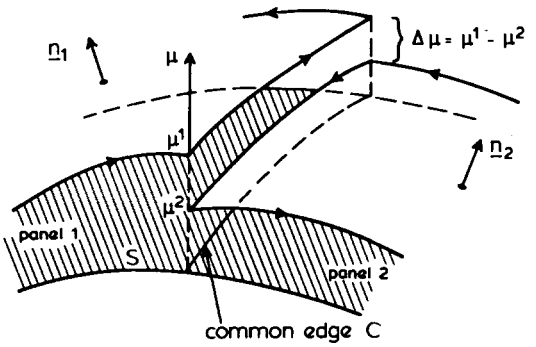

Fig. 3. Two adjacent panels.

and $\mathbf{v}_v$ can be written as

$$\mathbf{v}_v = \begin{pmatrix} u_v \\ v_v \\ w_v \end{pmatrix} = \begin{pmatrix} w_s(\sigma = \gamma_2) - v_s(\sigma = \gamma_3) \\ u_s(\sigma = \gamma_3) - w_s(\sigma = \gamma_1) \\ v_s(\sigma = \gamma_1) - u_s(\sigma = \gamma_2) \end{pmatrix}. \tag{6.3}$$

The velocity components of a surface vortex distribution can thus be written in terms of the velocity due to a surface source distribution. To obtain the same order of truncation error as with a source distribution, $\gamma = \nabla\mu \times \mathbf{n}$ has to be of the same order of accuracy as σ, and therefore μ itself has to be one order higher.

The line integral in (6.1) stems from the discontinuity of the dipole strength at panel edges. In the interior of the surface S the two line-vortex contributions of the common edge of two adjacent panels represent a single line-vortex contribution with line-vortex strength $\Delta\mu$, i.e. the jump in μ across the common edge (Fig. 3). The contribution from this line vortex is spurious since analytically the dipole μ does not jump across the edge: the line-vortex contributions cancel each other exactly. Therefore this line-vortex contribution is entirely due to the discretization of μ and is of the order of the truncation error of $\mathbf{v}_v$ (as will be shown), and therefore should be neglected in the interior of S. If it is known in advance that the boundary S of the computational domain Ω is closed and μ is continuous in all ξ on S, then the line-vortex integral can be omitted entirely from equation (6.1).

The line vortex has to be taken into account whenever the term is not caused by the discretization, that is, at the boundary of a nonclosed surface S, and along curves in the interior of S where μ is discontinuous. Then the line-vortex contribution is:

$$\mathbf{v}_{lv}(\mathbf{x}) = \oint_c -\mu \frac{\mathbf{r} \times \mathrm{d}\mathbf{l}}{r^3} = \sum_i \int_{c_i} -\mu \frac{\mathbf{r} \times \mathrm{d}l}{r^3}, \tag{6.4}$$

where the line integral is taken along a C^0-continuous curve $C = \Sigma_i C_i$. The position of a curve C_i is expressed in terms of a local coordinate system with origin at M on C_i and with unit direction vectors $\mathbf{t}$, $\mathbf{n} \times \mathbf{t}$ and $\mathbf{n}$ (Appendix I, Fig. I.2) where $\mathbf{t}$ is tangent to C_i at M and $\mathbf{n}$ is the normal at M of the surface ΔS.

Now ξ on C_i is given by (Appendix I, equation (I.6))

$$\xi = \xi t + \tfrac{1}{2}\kappa_g \xi^2(\mathbf{n} \times \mathbf{t}) + \tfrac{1}{2}\kappa_n \xi^2 \mathbf{n} + \lambda_g \xi^3(\mathbf{n} \times \mathbf{t}) + \lambda_n \xi^3 \mathbf{n} + \ldots \tag{6.5}$$

where κ_g, κ_n, . . . are assumed to be of O(1) at most.

In terms of the local coordinate system

$$\mathbf{e}_1' = \mathbf{t}, \quad \mathbf{e}_2' = \mathbf{n} \times \mathbf{t}, \quad \mathbf{e}_3' = \mathbf{n}, \tag{6.6}$$

we have

$$\mathbf{dl} = \mathrm{d}\xi, \tag{6.7}$$

and

$$\begin{aligned} \mathbf{r} = \mathbf{x} - \xi &= \mathbf{r}_f' + \tfrac{1}{2}\xi^2(\kappa_g \mathbf{e}_2' + \kappa_n \mathbf{e}_3') + \xi^3(\lambda_g \mathbf{e}_2' + \lambda_n \mathbf{e}_3') + \mathrm{O}(\Delta^4) \\ &= \mathbf{r}_f' + \mathbf{r}_{c2} + \mathbf{r}_{c3} + \mathrm{O}(\Delta^4). \end{aligned} \tag{6.8}$$

where $\mathbf{r}_f'$ is the distance from the field point $\mathbf{x}$ to the tangent line,

$$\mathbf{r}_f' = \mathbf{x} - \xi \mathbf{e}_1'. \tag{6.9}$$

Expanding $1/r^3$ as follows:

$$\frac{1}{r^3} = \frac{1}{r_f'^3}(1 + C_1 + C_2 + \mathrm{O}(\Delta^3)), \tag{6.10}$$

and

$$\mu(\xi) = \mu_0 + \mu_1 + \mu_2 + \mathrm{O}(\Delta^3), \tag{6.11}$$

we have

$$\begin{aligned} \int_{c_i} -\mu \frac{\mathbf{r} \times \mathbf{dl}}{r^3} = \int_{c_i} &-(\mu_0 + \mu_1 + \mu_2 + \ldots)\frac{1}{r_f'^3}(1 + C_1 + C_2 + \mathrm{O}(\Delta^3)) \\ &\times [(\mathbf{r}_f' + \mathbf{r}_{c2} + \mathbf{r}_{c3} + \mathrm{O}(\Delta^4)) \times \mathrm{d}\xi]. \end{aligned} \tag{6.12}$$

The leading terms in the expansion are

$$\mathbf{L}_1 = \int_{c_i} -\mu_0 \frac{\mathbf{r}_f' \times \mathrm{d}\xi}{r_f'^3} = \mathrm{O}\left(\frac{1}{\Delta}\right),$$

$$\mathbf{L}_2 = \int_{c_i} -\mu_0 \frac{1}{r_f'^3} C_1 \mathbf{r}_f' \times \mathrm{d}\xi = \mathrm{O}(1),$$

$$\mathbf{L}_3 = \int_{c_i} -\mu_0 \frac{1}{r_f'^3} \mathbf{r}_{c2} \times \mathrm{d}\xi = \mathrm{O}(1),$$

$$\mathbf{L}_4 = \int_{c_i} -\mu_1 \frac{1}{r_f'^3}\mathbf{r}_f' \times \mathrm{d}\boldsymbol{\xi} = \mathrm{O}(1),$$

$$\mathbf{L}_5 = \int_{c_i} -\mu_0 \frac{1}{r_f'^3}\mathrm{C}_2\mathbf{r}_f' \times \mathrm{d}\boldsymbol{\xi} = \mathrm{O}(\Delta),$$

$$\mathbf{L}_6 = \int_{c_i} -\mu_0 \frac{1}{r_f'^3}\mathrm{C}_1\mathbf{r}_{c2} \times \mathrm{d}\boldsymbol{\xi} = \mathrm{O}(\Delta),$$

$$\mathbf{L}_7 = \int_{c_i} -\mu_0 \frac{1}{r_f'^3}\mathbf{r}_{c3} \times \mathrm{d}\boldsymbol{\xi} = \mathrm{O}(\Delta),$$

$$\mathbf{L}_8 = \int_{c_i} -\mu_1 \frac{1}{r_f'^3}\mathrm{C}_1\mathbf{r}_f \times \mathrm{d}\boldsymbol{\xi} = \mathrm{O}(\Delta),$$

$$\mathbf{L}_9 = \int_{c_i} -\mu_1 \frac{1}{r_f'^3}\mathbf{r}_{c2} \times \mathrm{d}\boldsymbol{\xi} = \mathrm{O}(\Delta),$$

$$\mathbf{L}_{10} = \int_{c_i} -\mu_2 \frac{1}{r_f'^3}\mathbf{r}_f \times \mathrm{d}\boldsymbol{\xi} = \mathrm{O}(\Delta). \tag{6.13}$$

The other terms are at least $\mathrm{O}(\Delta^2)$. To achieve a second-order truncation error all integrals $\mathbf{L}_1 - \mathbf{L}_{10}$ should be taken into account.

To show that the line integral can be neglected in the interior of S we will consider two adjacent panels, 1 and 2, with common edge C (Fig. 3). The total line-integral contribution of C is:

$$\int_c -\mu^1 \frac{\mathbf{r} \times \mathrm{d}\mathbf{l}}{r^3} - \int_c -\mu^2 \frac{\mathbf{r} \times \mathrm{d}\mathbf{l}}{r^3} = \int_c -\Delta\mu \frac{\mathbf{r} \times \mathrm{d}\mathbf{l}}{r^3} \tag{6.14}$$

with μ^i the dipole strength of panel i along C. The minus sign in front the second integral in (6.14) is due to the fact that C is traversed in opposite direction.

A polynomial approximation of μ of order p gives for $\boldsymbol{\xi}$ on C:

$$\mu^1(\boldsymbol{\xi}) = \mu_{\text{exact}}(\boldsymbol{\xi}) + \mathrm{O}(\Delta^{p+1}),$$

$$\mu^2(\boldsymbol{\xi}) = \mu_{\text{exact}}(\boldsymbol{\xi}) + \mathrm{O}(\Delta^{p+1}),$$

and

$$(\Delta\mu)_0(\boldsymbol{\xi}) = \mathrm{O}(\Delta^{p+1}),$$

$$(\Delta\mu)_1(\boldsymbol{\xi}) = \mathrm{O}(\Delta^{p}), \tag{6.15}$$

$$(\Delta\mu)_2(\boldsymbol{\xi}) = \mathrm{O}(\Delta^{p-1}).$$

Substituting $\Delta\mu$ for μ in (6.13) then shows that the line-vortex contribution is $O(\Delta^p)$. Since the approximation of the velocity due to the surface-vortex distribution involves the same truncation error, that is $O(\Delta^p)$, it is clear that the contribution (6.14) can be neglected.

Far field: $r_f = O(1)$

Expansion of the surface vorticity integral gives

$$\begin{aligned} \mathbf{v}_d(\mathbf{x}) &= \mathbf{v}_v(x) = \iint_{\Delta S} \gamma \times \frac{\mathbf{r}}{r^3}\, dS \\ &= -\mu_x \frac{\mathbf{e}_2 \times \mathbf{x}}{r_0^3} M_{00} + \mu_y \frac{\mathbf{e}_1 \times \mathbf{x}}{r_0^3} M_{00} + O(\Delta^4). \end{aligned} \tag{6.16}$$

7. Potential due to a dipole distribution

Near field: $r_f = O(\Delta)$

The potential due to a dipole distribution on a panel Δs is given by

$$\phi_d(\mathbf{x}) = -\iint_{\Delta S} \frac{\mu}{r^3} (\mathbf{n} \cdot \mathbf{r})\, dS, \tag{7.1}$$

and is expanded as follows:

$$\begin{aligned} \phi_d(\mathbf{x}) &= -\iint_{\Delta S} \frac{\mu}{r^3} (\nabla \mathbf{F} \cdot \mathbf{r})\, dA \\ &= -\iint_{\Delta S} \frac{1}{r_f^3} (1 + C_{31} + C_{32} + \dots)(\mu_0 + \mu_1 + \mu_2 + \dots)(-\zeta_\xi (x - \xi) \\ &\quad -\zeta_\eta (y - \eta) + (z - \zeta))\, dA \\ &= K_1 + (K_2 + K_3 + K_4) + (K_5 + \cdots + K_{10}) + O(\Delta^3). \end{aligned} \tag{7.2}$$

The leading terms in the expansion are

$$K_1 = -\iint_{\Delta S} \frac{1}{r_f^3} \mu_0 z\, dA = O\left(\frac{1}{r_f^3} z \Delta^2\right) = O(1),$$

$$K_2 = -\iint_{\Delta S} \frac{1}{r_f^3} \mu_0 (-\zeta_{2\xi}(x - \xi) - \zeta_{2\eta}(y - \eta) - \zeta_2)\, dA = O(\Delta),$$

$$K_3 = -\iint_{\Delta S} \frac{1}{r_f^3} \mu_0 C_{31} z\, dA = O\left(\frac{1}{r_f^3} \frac{\Delta^2 z^2}{r_f^2} \Delta^2\right) = O(\Delta),$$

$$
\begin{aligned}
K_4 &= -\iint_{\Delta S} \frac{1}{r_f^3}\,\mu_1 z\,\mathrm{d}A = \mathrm{O}\left(\frac{\Delta z}{r_f^3}\,\Delta^2\right) &&= \mathrm{O}(\Delta),\\
K_5 &= -\iint_{\Delta S} \frac{1}{r_f^3}\,\mu_0(-\zeta_{3\xi}(x-\xi) - \zeta_{3\eta}(y-\eta) - \zeta_3)\,\mathrm{d}A &&= \mathrm{O}(\Delta^2),\\
K_6 &= -\iint_{\Delta S} \frac{1}{r_f^3}\,\mu_0 C_{31}(-\zeta_{2\xi}(x-\xi) - \zeta_{2\eta}(y-\eta) - \zeta_2)\,\mathrm{d}A &&= \mathrm{O}(\Delta^2),\\
K_7 &= -\iint_{\Delta S} \frac{1}{r_f^3}\,\mu_0 C_{32} z\,\mathrm{d}A = \mathrm{O}\left(\frac{z^2\Delta^5}{r_f^5}, \frac{z^3\Delta^6}{r_f^7}, \frac{z\Delta^6}{r_f^5}\right) &&= \mathrm{O}(\Delta^2),\\
K_8 &= -\iint_{\Delta S} \frac{1}{r_f^3}\,\mu_1(-\zeta_{2\xi}(x-\xi) - \zeta_{2\eta}(y-\eta) - \zeta_2)\,\mathrm{d}A &&= \mathrm{O}(\Delta^2),\\
K_9 &= -\iint_{\Delta S} \frac{1}{r_f^3}\,\mu_1 C_{31} z\,\mathrm{d}A = \mathrm{O}\left(\frac{\Delta^3 z^2}{r_f^5}\,\Delta^2\right) &&= \mathrm{O}(\Delta^2),\\
K_{10} &= -\iint_{\Delta S} \frac{1}{r_f^3}\,\mu_2 z\,\mathrm{d}A = \mathrm{O}\left(\frac{\Delta^2 z}{r_f^3}\,\Delta^2\right) &&= \mathrm{O}(\Delta^2). \qquad (7.3)
\end{aligned}
$$

The other terms are least third order in Δ.

It is clear that the computation of the velocity potential due to a dipole distribution involves much more work than that due to a source distribution to obtain the same level of accuracy. E.g. a constant source and flat panel representation gives an $O(\Delta^2)$ truncation error, whereas a linear dipole and a quadratic panel is needed to obtain the same order of truncation error (integrals I_1 and K_1–K_4 have to be calculated respectively).

It is well known, however, that for smooth boundaries a piecewise constant dipole distribution on a flat panel will given an $O(\Delta^2)$ truncation error, and not an $O(\Delta)$ error as is suggested by the analysis of the integrals.

To explain this we take a closer look at the expansion (7.2). The integrals K_1, K_4, K_{10} are the leading terms of the expansion of the integral

$$\tilde{K}_1 = -\iint_{\Delta S} \frac{1}{r_f^3}\,\mu z\,\mathrm{d}A. \qquad (7.4)$$

For smooth boundaries $z = O(\Delta^2)$ and all terms are one order higher than given in (7.3) which is the general case where z is assumed to be $O(\Delta)$. Therefore K_1 is $O(\Delta)$, K_4 is $O(\Delta^2)$, and K_{10} is $O(\Delta^3)$. The integrals K_2, K_3, K_5 are the leading terms of the expansion of the integral

$$\tilde{K}_2 = \mu_0 \iint_{\Delta S} -\frac{1}{r_f^3}\left(\frac{3z^2}{r_f^2} - 1\right)\zeta - \frac{1}{r_f^3}(-\zeta_\xi(x-\xi) - \zeta_\eta(y-\eta))\,\mathrm{d}A, \qquad (7.5)$$

which can be written as

$$\tilde{K}_2 = -\mu_0 \oint_c \frac{\zeta}{r_f^3}\,[(y-\eta)\,\mathrm{d}\xi - (x-\xi)\,\mathrm{d}\eta]. \qquad (7.6)$$

If the geometry is smooth and ζ_{exact} is approximated by $\zeta = \zeta_{exact} + O(\Delta^p)$, then the truncation error of the approximation of (7.5) is of $O(\Delta^{p-1})$. However, if we consider two adjacent panels and use an argument similar to that applied in Section 6 to the line-vortex contribution, μ_0 in the integral (7.6) can be replaced by the jump $\Delta\mu$ in μ_0 which is of $O(\Delta)$ if μ is assumed to be continuous. Thus the truncation error of the combined contribution $\tilde{K}_2$ of two adjacent panels is of $O(\Delta^p)$. This means that all terms in the expansion of $\tilde{K}_2$ are one order higher if combined with the similar terms of $\tilde{K}_2$ of the adjacent panels. So that in obtaining a second-order truncation error K_2 and K_3 can be neglected.

Far field: $r_f = O(1)$

In this case expanding (7.1) gives

$$\phi_d(\mathbf{x}) = -\iint_{\Delta S} \frac{\mu_0}{r_0^3} z \, dA + O(\Delta^4)$$

$$= -\frac{\mu_0 z}{r_0^3} M_{00} + O(\Delta^4). \tag{7.7}$$

8. Truncation errors due to panel boundary approximation

The area of integration ΔA_i of a panel ΔS_i is obtained by projecting the curved surface ΔS_i along the local normal $\mathbf{n}_i$ onto the ξ,η-plane. The boundaries of ΔA_i are projections of parts of the space curves $\mathbf{x}(u, v)$ with $u = u_i$, $u = u_{i+1}$, $v = v_j$ and $v = v_{j+1}$, and therefore they are curved in general. Usually these four boundaries are approximated by straight line segments forming a quadrilateral panel as shown in Fig. 4. This approximation introduces an additional truncation error.

To investigate the order of magnitude of this error two adjacent panels are considered (see Fig. 5). The common edge of the panels ΔS_{i-1} and ΔS_i is the curve $\mathbf{x}(u_i, v)$ with $v \in [v_j, v_{j+1}]$. For panel ΔS_{i-1} this curve is projected along $\mathbf{n}_{i-1}$, whereas it is projected along $\mathbf{n}_i$ for panel

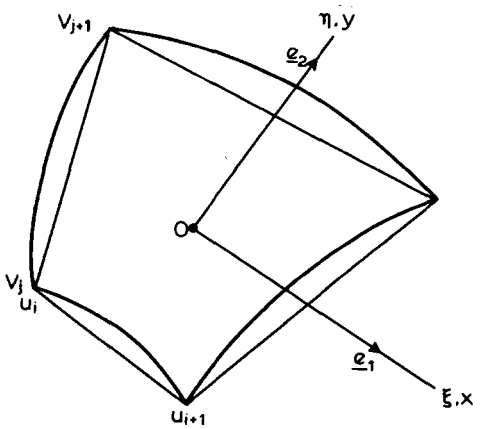

Fig. 4. Curved boundaries of ΔA.

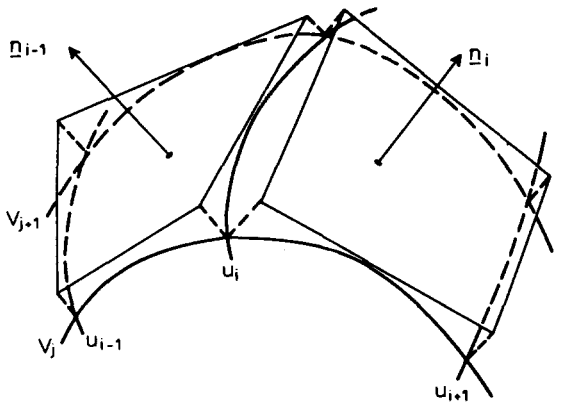

Fig. 5. Gaps between adjacent panels due to projection along normals.

ΔS_i to form the boundaries of the respective integration areas ΔA_{i-1} and ΔA_i. If the exact integration areas are used (i.e., with the curved boundary in the plane $\zeta = 0$) the panels abut to the order of accuracy indicated by the analysis in the previous sections. But using the straight line approximations the panels do not abut whatever normal curvature terms are included. The projections of the straight line areas along there respective normals onto the surface will leave a gap on the surface between the panels.

To deduce the order of magnitude of the error caused by the straight-line approximation of the panel boundaries, we decompose the surface curvature into normal curvature and geodesic ("internal") curvature (Appendix I). When we have a flat surface and curved lines of constant u and v within the surface, we have only geodesic curvature. Since the lines $u = u_i$, etc. are curved, the straight line approximation introduces an error in the panel surface approximation. In general the gap due to geodesic curvature has width $O(\Delta^2)$, and area $O(\Delta^3)$, (see equation (I.15). Appendix I). The error due to the geodesic curvature is cancelled when the gap is *between* two panels; e.g., a flat disk can be approximated exactly by flat panels with straight line segments, except for the error at the edge of the disk. Therefore geodesic curvature only has to be taken into account at surface edges. But we also have a contribution due to the normal curvature, present when the surface itself is curved. Clearly this curvature also induces curved boundaries of the area of integration ΔA_i. The gap due to *normal curvature* has width $O(\Delta^3)$, and area $O(\Delta^4)$, (see (I.15), Appendix I).

The lowest-order terms in the potential and velocity-potential expansions are $O(1/\Delta^2)$ times area of integration. Thus, when using straight boundaries the truncation error will be $O(\Delta^{-2}\Delta^3) = O(\Delta)$ due to geodesic curvature, and $O(\Delta^{-2}\Delta^4) = O(\Delta^2)$ due to normal curvature. Therefore corrections are needed for the lower-order terms to achieve higher-order truncation errors.

9. Conclusions

We will now summarize the results obtained in the previous sections. Using Taylor series expansions for the source distribution σ, the dipole distribution μ and the panel surface ζ, the surface integrals of the boundary integral equations (1.2) and (1.3) were expanded in series of integrals which can be calculated analytically. Estimates of the local truncation

Table 1. Summary of results on local errors

	Local trunc. error ε_Δ	σ	μ	Panel geometry
int. eq.				
$\phi(\mathbf{x})$	$O(\Delta^2)$	const.	lin.	quadr.
S non-smooth	$O(\Delta^3)$*	lin.	quadr.	cubic
int. eq.				
$\phi(\mathbf{x})$	$O(\Delta^2)$	const.	lin.	flat
S smooth	$O(\Delta^3)$*	lin.	quadr.	quadr.
int. eq.				
$\mathbf{v}(\mathbf{x})$	$O(\Delta)$	const.	lin.	flat
S smooth or non-smooth	$O(\Delta^2)$*	lin.	quadr.	quadr.

* To obtain this local truncation error the panel boundaries have to be approximated using higher-order representations for the lowest-order terms in the expansions (Section 8).

errors were derived by estimating the order of magnitude of the integrals in terms of the characteristic panel size Δ. The velocity is the physical quantity of interest in most applications, and it can be obtained either by using (1.3), giving $\mathbf{v}(\mathbf{x})$ directly, or by using (1.2), giving the potential $\phi(\mathbf{x})$, from which $\mathbf{v}(\mathbf{x})$ can be calculated using numerical differentiation. Therefore $\phi(\mathbf{x})$ should be approximated one order higher than $\mathbf{v}(\mathbf{x})$.

Table 1 summarizes the main results of the estimates. It shows the minimum approximations needed for the source σ, the dipole μ and the panel geometry to obtain a given order for the local truncation error ε_Δ. It is assumed that the boundary S is closed and that μ is continuous in every ξ on S. Only the two lower-order consistent approximations are shown for both the potential equation (1.2) and the velocity equation (1.3). Notice that in all cases the dipole μ should be approximated one order higher than the source σ.

In general it can be concluded from this analysis that the use of equation (1.2) will require more effort to obtain a given accuracy in the velocity $\mathbf{v}(\mathbf{x})$. However, one should keep in mind that this is a *local* error analysis, and not a *global* error analysis. In future we hope to get some answers on the relation between local and global errors to be able to predict the asymptotic behaviour of the errors in the solutions obtained using these panel methods, to solve Laplace's equation.

Acknowledgements

The author wishes to thank B. Oskam and H.W.M. Hoeijmakers of the National Aerospace Laboratory NLR, The Netherlands, for many interesting contributions and discussions, as well as P.J. Zandbergen of the University of Twente for his valued encouragement.

The investigations were supported by the Netherlands Technology Foundation (STW), by the University of Twente, and by Delft Hydraulics.

Appendix I. Curves on surfaces in space

Let $\mathbf{r} = \mathbf{r}(u)$ define a C^2-continuous curve C on a C^2-continuous surface S (u is the arc length measured from some fixed point on the curve C). Then the unit tangent $\mathbf{t}_c$, the unit normal

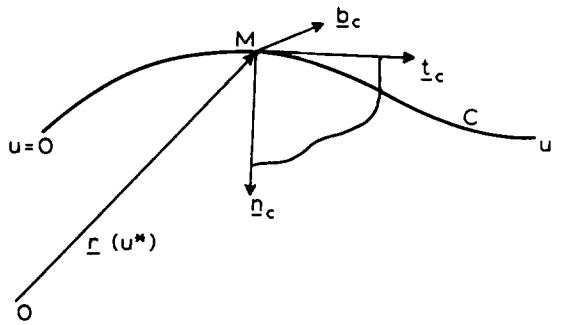

Fig. I.1. Definition of $\mathbf{t}_c$, $\mathbf{n}_c$ and $\mathbf{b}_c$.

$\mathbf{n}_c$ and the unit binormal $\mathbf{b}_c$ in $\mathbf{r}(u^*) = M$ on C are

$$\mathbf{t}_c = \frac{\mathrm{d}\mathbf{r}}{\mathrm{d}u}, \tag{I.1}$$

$$\mathbf{n}_c = \frac{\mathrm{d}\mathbf{t}_c}{\mathrm{d}u} \Big/ \left|\frac{\mathrm{d}\mathbf{t}_c}{\mathrm{d}u}\right| = \frac{1}{\kappa}\frac{\mathrm{d}\mathbf{t}_c}{\mathrm{d}u}, \tag{I.2}$$

$$\mathbf{b}_c = \mathbf{t}_c \times \mathbf{n}_c. \tag{I.3}$$

The vector $\mathbf{n}_c$ is orthogonal to $\mathbf{t}_c$ and lies in the osculating plane at $\mathbf{r}$ pointing in the direction of concavity of the curve (Fig. I.1): the quantity κ is called the curvature of the curve C at $\mathbf{r}(u^*)$, sometimes referred to as $1/\varrho$. Generally $\mathbf{n}_c$ is not normal to the surface S at M, but $\mathbf{n}_c$ can be decomposed in terms of the normal $\mathbf{n}$ of S in M and $\mathbf{n} \times \mathbf{t}$ (Fig. I.2), with $\mathbf{t} = \mathbf{t}_c$:

$$\mathbf{n}_c = \frac{\kappa_n}{\kappa}\mathbf{n} + \frac{\kappa_g}{\kappa}\mathbf{n} \times \mathbf{t}. \tag{I.4}$$

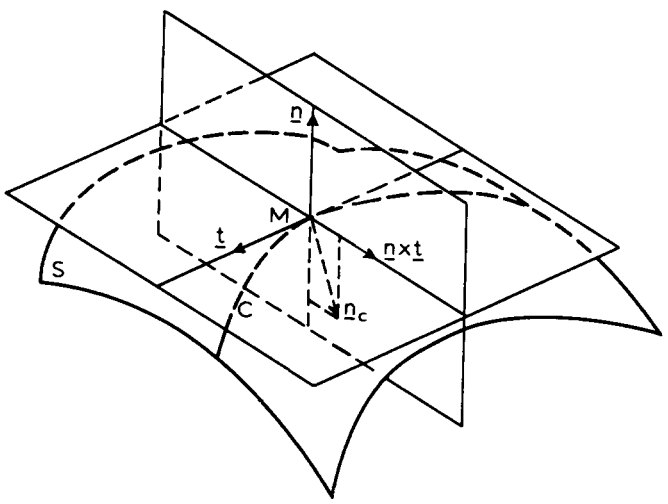

Fig. I.2. Curve C on S.

The coefficient κ_n is the normal curvature of S in M and κ_g the geodesic (internal) curvature of S. κ, κ_n and κ_g are related by

$$\kappa^2 = \kappa_n^2 + \kappa_g^2. \tag{I.5}$$

Introduce the local coordinate system $\langle \mathbf{t}, \mathbf{n} \times \mathbf{t}, \mathbf{n} \rangle$ with origin in $\mathbf{r} = M$ on C. Locally C may be written as ($\boldsymbol{\xi}$ on C)

$$\begin{aligned} \boldsymbol{\xi} &= \xi \mathbf{t} + \eta(\mathbf{n} \times \mathbf{t}) + \zeta \mathbf{n} \\ &= \xi \mathbf{t} + (\tfrac{1}{2}\kappa_g \xi^2 + \lambda_g \xi^3 + \dots)\mathbf{n} \times \mathbf{t} + (\tfrac{1}{2}\kappa_n \xi^2 + \lambda_n \xi^3 + \dots)\mathbf{n}. \end{aligned} \tag{I.6}$$

Also S may be written as ($\mathbf{x}$ on S)

$$\mathbf{x} = x\mathbf{t} + y(\mathbf{n} \times \mathbf{t}) + z\mathbf{n}, \tag{I.7}$$

or

$$z = c_{xx}x^2 + c_{xy}xy + c_{yy}y^2 + \cdots \tag{I.8}$$

where $c_{xx} = \kappa_n$.

Now let $\mathbf{x}_0 = (x_0, y_0, z_0)^T$ be on S, with x_0 and y_0 $O(\Delta)$:

$$\left.\begin{aligned} x_0 &= a_1\Delta \\ y_0 &= a_2\Delta \end{aligned}\right\} \Rightarrow z_0 = a_3\Delta^2. \tag{I.9}$$

We now project the line segment L of C:

$$\mathbf{r}(u),\ u \in [u^* - a, u^* + b](a, b = O(\Delta))$$

on the plane

$$\mathbf{n}' \cdot \mathbf{x}' = 0, \tag{I.10}$$

where $\mathbf{n}'$ is the local normal of S at $\mathbf{x}_0$ and $\mathbf{x}' = (x', y', z')$ is expressed in the local coordinate system at $\mathbf{x}_0$: $\langle \mathbf{t}', \mathbf{n}' \times \mathbf{t}', \mathbf{n}' \rangle$. (See Fig. I.3). Now

$$\begin{aligned} \mathbf{n}' &= (n_1\Delta + O(\Delta^2))\mathbf{t} + (n_2\Delta + O(\Delta^2))\mathbf{n} \times \mathbf{t} + (1 - n_3\Delta + O(\Delta^2))\mathbf{n}, \\ \mathbf{n}' \times \mathbf{t}' &= (s_1\Delta + O(\Delta^2)\mathbf{t} + (1 - s_2\Delta + O(\Delta^2))\mathbf{n} \times \mathbf{t} + (s_3\Delta + O(\Delta^2))\mathbf{n}, \\ \mathbf{t}' &= (1 - t_1\Delta + O(\Delta^2))\mathbf{t} + (t_2\Delta + O(\Delta^2))\mathbf{n} \times \mathbf{t} + (t_3\Delta + O(\Delta^2))\mathbf{n} \end{aligned} \tag{I.11}$$

and

$$\begin{aligned} \mathbf{t} &= (1 - t_1\Delta + O(\Delta^2))\mathbf{t}' + (s_1\Delta + O(\Delta^2))\mathbf{n}' \times \mathbf{t}' + (n_1\Delta + O(\Delta^2))\mathbf{n}', \\ \mathbf{n} \times \mathbf{t} &= (t_2\Delta + O(\Delta^2))\mathbf{t}' + (1 - s_2\Delta + O(\Delta^2))\mathbf{n}' \times \mathbf{t}' + (n_2\Delta + O(\Delta^2))\mathbf{n}', \\ \mathbf{n} &= (t_3\Delta + O(\Delta^2))\mathbf{t}' + (s_3\Delta + O(\Delta^2))\mathbf{n}' \times \mathbf{t}' + (1 - n_3\Delta + O(\Delta^2))\mathbf{n}'. \end{aligned}$$

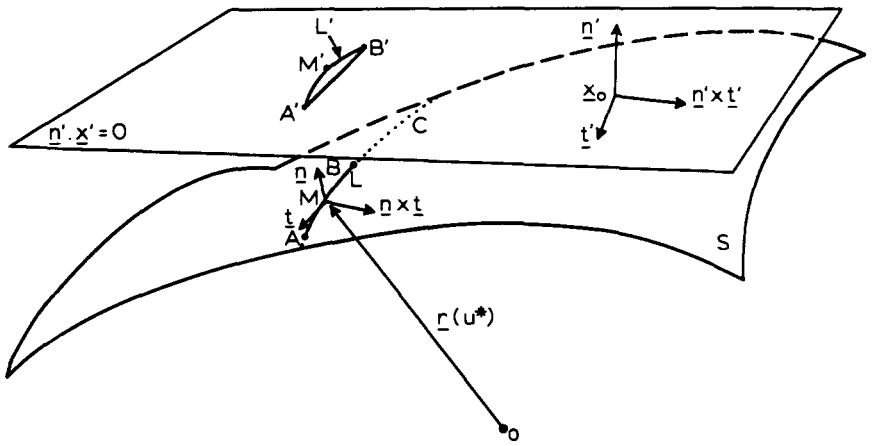

Fig. I.3. Projection L' of L on $\mathbf{n}' \cdot \mathbf{x}' = 0$.

In the new coordinate system L can be written as (from (I.6))

$$\begin{aligned}\xi' &= \xi'_0 + \xi[(1 - t_1\Delta + O(\Delta^2))\mathbf{t}' + (s_1\Delta + O(\Delta^2))\mathbf{n}' \times \mathbf{t}' + (n_1\Delta + O(\Delta^2))\mathbf{n}'] \\ &\quad + \tfrac{1}{2}\kappa_g\xi^2[(t_2\Delta + O(\Delta^2))\mathbf{t}' + (1 - s_2\Delta + O(\Delta^2))\mathbf{n}' \times \mathbf{t}' + (n_2\Delta + O(\Delta^2))\mathbf{n}'] \\ &\quad + \tfrac{1}{2}\kappa_n\xi^2[(t_3\Delta + O(\Delta^2))\mathbf{t}' + (s_3\Delta + O(\Delta^2))\mathbf{n}' \times \mathbf{t}' + (1 - n_3\Delta + O(\Delta^2))\mathbf{n}'] \\ &\quad + O(\Delta^3)(\mathbf{n}' \times \mathbf{t}') + O(\Delta^3)\mathbf{n}', \end{aligned} \tag{I.13}$$

or

$$\begin{aligned}\xi' &= \xi'_0 \\ &\quad + \begin{pmatrix} \xi(1 - t_1\Delta + O(\Delta^2)) + (\tfrac{1}{2}\kappa_g\xi^2)t_2\Delta + (\tfrac{1}{2}\kappa_n\xi^2)t_3\Delta + O(\Delta^2\xi^2, \Delta\xi^3) \\ \xi(s_1\Delta + O(\Delta^2)) + (\tfrac{1}{2}\kappa_g\xi^2 + \lambda_g\xi^3)(1 - s_2\Delta) + (\tfrac{1}{2}\kappa_n\xi^2 + \lambda_n\xi^3)(s_3\Delta) \\ \qquad + O(\Delta^2\xi^2, \Delta\xi^3) \\ \xi(n_1\Delta + O(\Delta^2)) + (\tfrac{1}{2}\kappa_g\xi^2)n_2\Delta + (\tfrac{1}{2}\kappa_n\xi^2 + \lambda_n\xi^3)(1 - n_3\Delta) + O(\Delta^2\xi^2, \Delta\xi^3) \end{pmatrix}, \end{aligned} \tag{I.14}$$

and L' becomes (after translation)

$$\begin{aligned}\xi'_{L'} &= [\xi(1 - t_1\Delta + O(\Delta^2)) + \tfrac{1}{2}\kappa_g\xi^2 t_2\Delta + \tfrac{1}{2}\kappa_n\xi^2 t_3\Delta + O(\Delta^2\xi^2, \Delta\xi^3)]\mathbf{t}' \\ &\quad + [\xi(s_1\Delta + O(\Delta^2)) + \tfrac{1}{2}\kappa_g\xi^2(1 - s_2\Delta) + \lambda_g\xi^3 + \tfrac{1}{2}\kappa_n\xi^2 s_3\Delta \\ &\quad + O(\Delta^2\xi^2, \Delta\xi^3)]\mathbf{n}' \times \mathbf{t}' + 0\,\mathbf{n}'. \end{aligned} \tag{I.15}$$

References

1. J.L. Hess and A.M.O. Smith, Calculation of nonlifting potential flow about arbitrary three-dimensional bodies. Douglas Aircraft Company, Rep. no. ES 40622, Long Beach, California (1962).
2. J.J. Connor and C.A. Brebbia (eds), *Betech 86*, Proc. 2nd Boundary Element Technology Conference held at M.I.T., Cambridge (Mass.); Southampton (UK): Computational Mechanics Publications (1986).
3. W.L. Wendland, Asymptotic accuracy and convergence, Chap. 9 in: C.A. Brebbia (ed.), *Progress in boundary element methods*, Vol. 1, London: Pentech Press (1981), pp. 289–313.
4. H. Schippers, Multiple grid methods for equations of the second kind with applications in fluid mechanics, Thesis, Mathematisch Centrum, Amsterdam (1982).
5. J.L. Hess, Review of integral-equation techniques for solving potential-flow problems with emphasis on the surface-source method, *Comp. Meth. Appl. Mech. Eng.* 5 (1975) 145–196.
6. H.W.M. Hoeijmakers, A panel method for the determination of the aerodynamic characteristics of complex configurations in linearized subsonic or supersonic flow, National Aerospace Laboratory, Rep. NLR TR 80124, Amsterdam (1980).